Observation of IMF and seasonal effects in the location of auroral substorm onset

K. Liou, P. T. Newell, D. G. Sibeck, and C.-I Meng

Applied Physics Laboratory, Johns Hopkins University, Laurel, Maryland

M. Brittnacher and G. Parks

Geophysics Program, University of Washington, Seattle

Abstract. We use Polar ultraviolet imager (UVI) and Wind observations to study the location of 648 well-defined Northern Hemisphere auroral breakups (substorm onsets) in response to interplanetary magnetic field (IMF) orientation and season. The most likely onset location is at 2230 MLT and 67° Λ_m with half-maximum widths of 3 hours of MLT and 2° Λ_m, respectively. The onset latitude depends primarily on IMF B_z, but also B_x: the onset latitude decreases for $B_x > 0$ or $B_z < 0$ and increases for $B_x < 0$ or $B_z > 0$. The onset longitude depends on season and IMF B_y. In summer, substorms tend to occur in the early evening at ~2200 MLT, whereas in winter they tend to occur near midnight at ~2300 MLT. The average summer-winter difference in the onset location is ~1 hour of MLT. Large B_y effects on the onset longitude occur only when B_x and B_y are small. Onset locations shift toward earlier local times for $B_y > 0$ and toward midnight for $B_y < 0$. The average onset local time is earliest (2200 MLT) for $B_y > 0$ in summer and latest (2330 MLT) for $B_y < 0$ in winter. These dependencies coincide with those previously reported for the evening sector ionospheric zonal flow reversal in response to IMF B_y and season, indicating that auroral breakups are most likely in regions of large velocity shears. A weak dependence of the MLT onset location on the IMF B_x is identified: for $B_x > 0$ the onset location shifts toward dusk when $B_y > 0$ but toward dawn when $B_y < 0$; the sense of this shift reverses for $B_x < 0$. An implication of the results is that auroral breakup is not conjugate.

1. Introduction

The auroral substorm onset (auroral breakup) is a sudden brightening of arcs, usually the ones that are the most equatorward of a discrete arc system, in the midnight sector prior to the so-called substorm expansion phase, during which the brightened onset arcs evolve explosively into a large-scale auroral disturbance termed "auroral bulge" [*Akasofu*, 1964]. The final stage of the auroral substorm is termed the recovery phase, which starts at the moment that the previously intensified aurora fades. Further research from more observations suggested that a substorm contains one more phase, the growth phase [*McPherron*, 1970], which precedes the substorm onset. Auroral signatures during growth phase include, but are not limited to, a gradual expansion of the polar cap [*Kauristie*, 1995] and an equatorward drift of quiet auroral arcs [e.g., *Starkov et al.*, 1971; *Vorobjev et al.*, 1976]. Additional details of auroral substorm morphology can be found from a recent review paper from *Elphinstone et al.* [1996, and references therein].

Auroral substorms can be observed over a wide range of local times at nightside auroral latitudes. However, the initiation of a substorm is quite localized and preferentially takes place in the premidnight region [e.g., *Craven and Frank*, 1991]. Owing to the transient and localized nature of substorm onsets, the physical onset location of a substorm may not be easily identified with sparse ground-based cameras, which typically have limited field of view, or satellite-borne imagers, which have low temporal resolutions, such as those aboard the DMSP (two per orbit) and DE-1 (12 min) satellites. Although the ultraviolet imager on board the Viking satellite can provide good temporal resolution down to 20 s and good spatial resolution of ~20 km, reports on substorm onset based on Viking data have been limited to case studies, probably owing to the short lifetime of the imager. The ultraviolet imager (UVI) aboard the Polar satellite has continuously taken auroral images for more than 3 years since its launch and provided more than 1 million images for many types of auroral research. The UVI imaging rate is ~37 s, and the spatial resolution is ~40 km at nadir [*Torr et al.*, 1995] (although wobble of the imager platform significantly degrades this). In this study, we will take the advantage of the large volume of returned UVI imagery to study the ionospheric location of substorm onsets (auroral breakups), in

particular under different IMF and seasonal conditions. Specific issues that will be addressed in this paper are as follows.

It has been reported that the Harang discontinuity (HD) [*Heppner*, 1972; *Harang*, 1946], loosely defined as a region of sharp reversal of ionospheric convection electric field in the evening sector, was observed progressively earlier/later in local time at subauroral latitudes in the Northern/Southern Hemispheres for increasingly positive B_y [*Rodger et al.*, 1984]. This interplanetary magnetic field (IMF) B_y associated shift is also confirmed by *Ruohoniemi and Greenwald* [1995], who analyzed HF radar data and reported that the reversal in the zonal velocity in the 67°-79° Λ_m (magnetic latitude) interval occurs 2.5 hours in MLT earlier for $B_y > 0$ than for $B_y < 0$. Interestingly, many ground-based measurements have also indicated that onset arcs appear to occur just equatorward of the Harang discontinuity [e.g., *Koskinen and Pulkkinen*, 1995; *Baumjohann et al.*, 1981; *Robinson and Vondrak*, 1990]. If the HD and auroral breakups are colocated, similar IMF B_y effects must exist on the local time of breakups. Statistical analysis of ionospheric onset locations in response of B_y is therefore important and necessary to justify these observations.

The nightside high-latitude convection patterns are also seasonally dependent. It has been shown that HD could be identified above 67° Λ_m in winter but not in summer [*de la Beaujardiere et al.*, 1991]. On the basis of observations from HF radar, *Ruohoniemi and Greenwald* [1995] showed that the zonal flow reversal occurred 2.5 hours of MLT earlier in summer than in winter. Interestingly, seasonal effects in the nightside convection can be comparable to that of the IMF [*Rich and Hairston*, 1994]. However, *Rodger et al.* [1984] did not find strong evidence of seasonal dependence in their subauroral measurements. Again, we will investigate this seasonal effect by analyzing a large set of auroral breakup locations.

The shape and the size of the auroral oval are affected by the IMF. A linear correlation between the size of the quiet auroral oval and simultaneous hourly IMF B_z values has been reported by *Holzworth and Meng* [1975, 1984]. The work of *Meng* [1979] indicated that the northern polar cap center position shifts dawnward (duskward) for $B_y > 0$ ($B_y < 0$) and shifts tailward (sunward) for $B_x > 0$ ($B_x < 0$). However, the motion of the oval in the noon-midnight direction associated with B_x was not studied by *Holzworth and Meng* [1984]. Using the reported data from *Holzworth and Meng* [1984] and the fact that B_x and B_y are strongly anticorrelated in the solar wind, *Cowley et al.* [1991] argued that for $B_x > 0$ the auroral oval and polar cap should be shifted tailward in the Northern Hemisphere and sunward in the Southern Hemisphere and vice versa for $B_x < 0$. More recently, *Nakai* [1987] found that the size of the oval in the midnight sector increases (decreases) for $B_y > 0$ and decreases (increases) for $B_y < 0$ for a positive (negative) dipole tilt angle. Since auroral substorms exclusively occur within the diffusive oval, their latitudinal onset locations should reveal similar IMF effects. These effects will also be reinvestigated here.

The outline of the rest of the paper is as follows. We first describe how we determined auroral substorm onsets from UVI images. In section 3 we will show the statistical locations of substorm onset in terms of magnetic location and latitude. In section 4 we correlate the onset locations with hourly IMF. Section 5 shows seasonal effects on the onset locations. A discussion is given in section 6 and is followed by a summary.

2. Determination of Auroral Substorm Onset

In this study, auroral breakups (substorm onsets) are visually identified on the basis of the classical auroral substorm scheme *Akasofu* [1964]. We simply look through a sequence of raw images from the UVI database. Once a substorm event is found, the nightside parts of the images are reformatted in the altitude-adjusted corrected geomagnetic (AACGM) coordinate system [*Baker and Wing*, 1989]. Normally, we examine processed auroral images for a time interval of ∼10 min before and after a tentative onset. A thorough inspection of the substorm process is performed to make sure that the onset is followed by a continuing poleward and zonal expansion of the substorm bulge (expansion
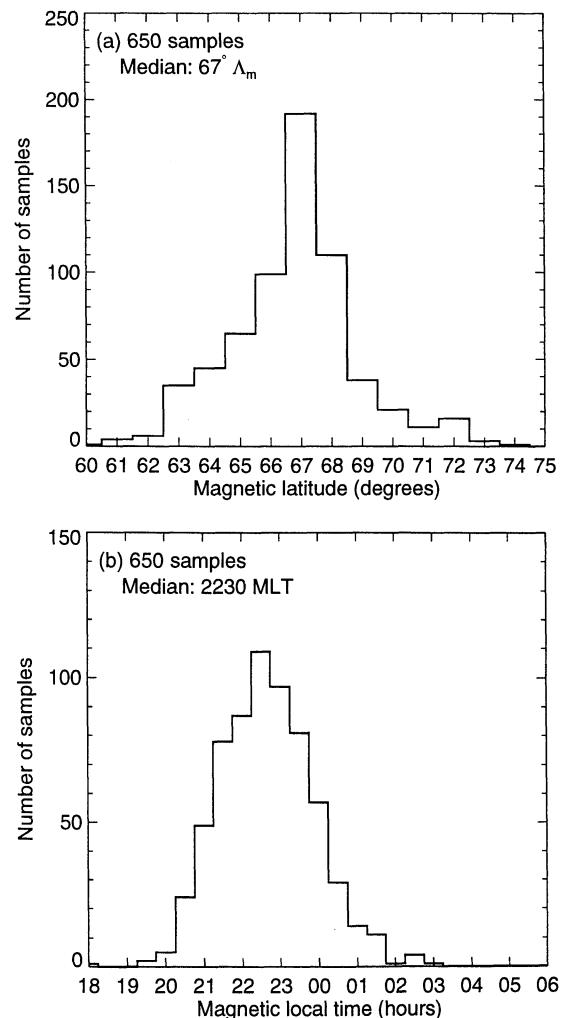
Figure 1. Histograms of auroral substorm onset location in 1° Λ_m increments for (a) magnetic latitude and in half-hour bins for (b) magnetic local time identified with Polar UVI images.

phase). This is done by tracing substorm features back in time and finding the first brightening (auroral breakup) in the oval. Once the onset image is determined, the location of onset is determined by the center of the onset arcs. The uncertainty for this type of onset determination is within ~ 1 min, which is not crucial to the present study because the center location of onset does not change dramatically within 1 min.

Our data set covers a period from March 30, 1996, to July 30, 1996, and from December 4, 1996, to May 31, 1997. A total of 648 substorm onsets with clear onset and expansion features was identified. We have also created auroral substorm movies in the MPEG format based on the list of 648 auroral substorm events. The movies have been made available directly to the public from our Web site at http//sd-www.jhuapl.edu/Auroral.

3. Distribution of Onset Location

Figures 1a and 1b show histograms of onset locations in terms of magnetic latitude and magnetic local time, respectively. A notable feature is the wide spread of onset locations in magnetic latitude and local time. The latitudinal location of onset sharply peaks at $67°$ Λ_m with a slowly decreasing tail that extends to low latitudes at $\sim 60°$ Λ_m. Substorm events drop sharply at latitudes higher than $\sim 69°$ Λ_m. Nonetheless, a few events can still be seen at latitudes as high as $74°$ Λ_m. The distribution width at the half maximum is $2°$ Λ_m. The median value for the latitudinal onset locations is estimated to be $67°$ Λ_m, and the mean is $66.6°$ Λ_m.

The magnetic local time distribution of substorm onsets (see Figure 1b) is near symmetric around 2230 MLT but with a longer tail extending to post midnight. The width of the distribution at the half-height is ~ 3.5 hours of MLT. Although a few events were observed as early as 1800 MLT or as late as 0300 MLT, it is estimated that 85% of the surveyed events occurred between 2100 and 2400 MLT (± 1.5 hours from 2230 MLT) and 70% of events occurred between 2130 and 2330 MLT (± 1 hour from 2230 MLT). The median value of onset locations is 2230 MLT, and the mean is slightly later at 2240 MLT.

4. IMF Effects

In this section we correlate auroral substorm onset locations with hourly averaged IMF data. Of the 648 onsets identified from the Polar UVI imagery, only 603 events have simultaneous IMF observations from the Wind spacecraft. IMF data were first propagated to the subsolar magnetopause by taking the solar wind speed and IMF into account [Liou et al., 1998]. The original 1-min IMF data are then averaged over a 1-hour period prior to onsets. Many previous studies have indicated that the auroral electrojet index AE correlates with the IMF B_z best when the IMF is shifted forward in time by 30 – 60 min [e.g., Meng et al., 1973; Arnoldy, 1971; Rostoker et al., 1972]; a shorter time response of 20 min is also obtained for AL and VB_s for strongly active intervals [Bargatze et al., 1986]. Therefore the hourly average of IMF is reasonable for the purpose of the present statistical analysis.
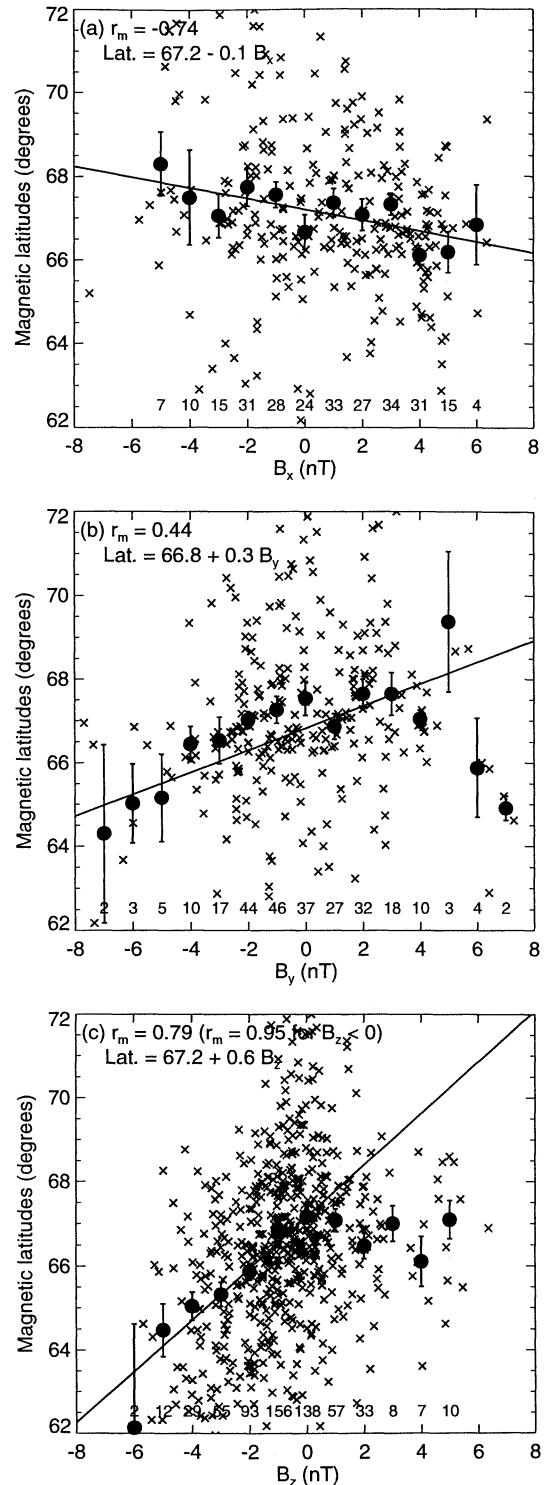
Figure 2. Dependence of latitudinal location of auroral substorm onset on (a) IMF B_x, (b) IMF B_y, and (c) IMF B_z. In each panel, error bars correspond to one standard deviation of the means, and numbers given at the bottom indicate the sample numbers for each bin. Light crosses overlaid in the background are the orginal data points.

4.1. Correlation of the Onset Latitude With IMF

We now consider IMF effects upon the location of onsets. Figures 2a-2c show the relationship between onset latitudes and the x, y, and z components of IMF, respectively.
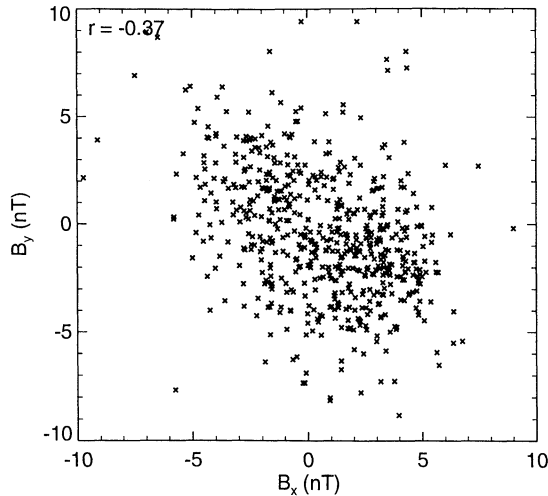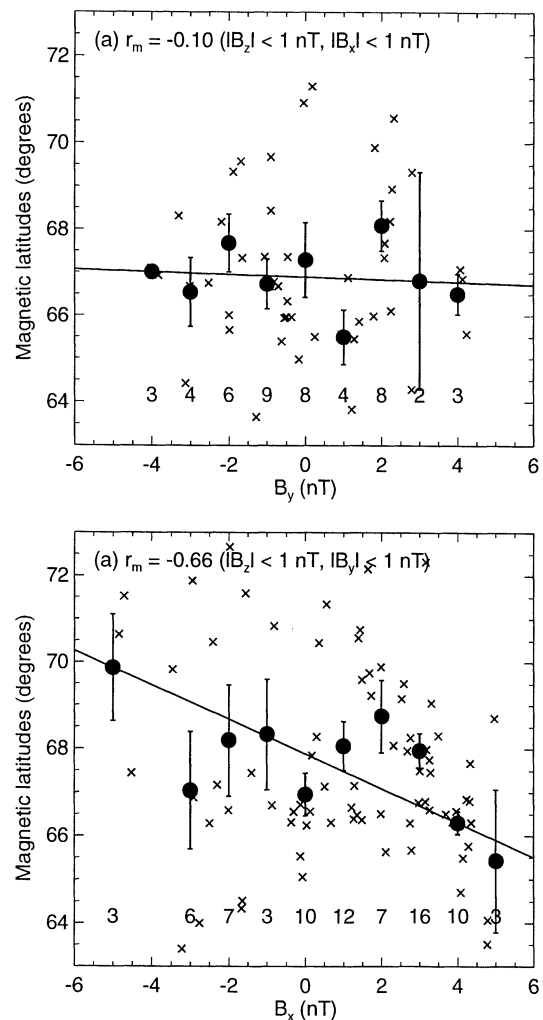
Figure 3. Correlation of the x and y components of the IMF for the surveyed 648 auroral substorm onset periods.

It is found from Figure 2c that our substorm onset events occurred predominately during southward IMF, indicating that a southward IMF is a preferred condition for substorms to occur and substorms can occur occasionally for northward IMF. Another interesting result is that the average location of onsets systematically moves equatorward as the IMF B_z becomes more negative (correlation coefficient of the means $r_m = 0.79$). Note that a higher correlation coefficient ($r_m = 0.95$) can be obtained if one considers negative B_z events only. The decreasing rate of the onset latitudes is estimated to be $0.6°/nT$ for $B_z < 0$, whereas there is slight turn-over for $B_z > 0$.
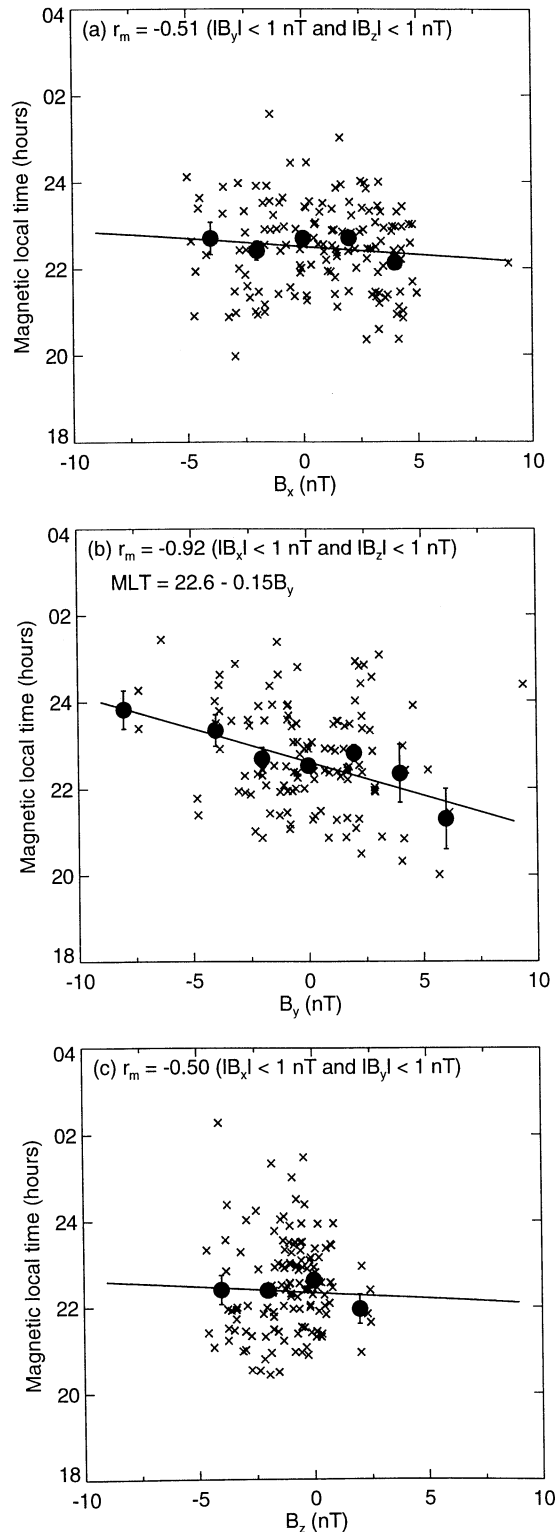
The relationship between the latitudinal location of onsets and the other two components of IMF, namely, B_x and B_y, is shown in Figures 2a and 2b. Since the size of the auroral oval is predominantly controlled by the z component of the IMF, a small B_z condition, $|B_z| < 1$ nT, is used to reduce the B_z effect. As expected, the correlation of the means is lower: $r_m = -0.74$ for B_x and $r_m = 0.44$ for B_y. One may argue that a small IMF $|B_z|$ implies a small dayside reconnection, and therefore this result does not apply to events when the effect of the dayside reconneciton is large. It is important to note that a small hourly IMF B_z does not mean the value of IMF B_z is small within the entire 1-hour-average period. It may correspond to a large negative B_z plus a large positive B_z that often precedes a southward turning of the IMF and sometimes occurs concurrently with the substorm onset. After all, most of the onset events occurred for small hourly IMF B_z (43% for $|B_z| < 1$ nT and 71% for $|B_z| < 2$ nT). Consistently, the tendency of the onset latitude with respect to the IMF B_x and B_y is very similiar for all IMF B_z events (not shown) except for a smaller correlation coefficient ($r_m = 0.51$ for B_x and $r_m = 0.38$ for B_y).

A combined result from Figures 2a and 2b indicates that an away sector ($B_x < 0$ and $B_y > 0$) results in a higher onset latitude than does a toward sector ($B_x > 0$ and $B_y < 0$). The somewhat smaller correlation from B_y is a bit surprising because the x and y components of IMF are normally highly correlated owing to the average Parker spiral config-

uration in the solar wind magnetic field. Consequently, any effect seen in B_x will also appear in B_y. Furthermore, on the basis of the framework of the "dipole plus uniform field" picture [*Dungey*, 1961; *Cowley*, 1973; *Stern*, 1973; *Lyons*, 1985], the Earth's dipole field lines, after reconnection, will be distorted in the same sense as the uniform field; therefore the latitudinal location of substorm onsets (occurring mainly in the premidnight region) should have a weak response to the y component of IMF but have a strong response to the x component. To justify these lines of argument, we have plotted the hourly values of B_x versus B_y in Figure 3 for all of the onset events studied. Indeed, the two IMF components for our survey periods were correlated, but not as high as normally seen in the solar wind (the correlation coefficient is $r = -0.37$). To isolate a pure B_x or a B_y effect, we have regenerated Figures 2a and 2b in Figures 4a and 4b, respectively, by limiting effects from the other two magnetic field components. For the B_y effect (Figure 4a), $|B_z| < 1$ nT and $|B_x| < 1$ nT conditions are used, and for the B_x effect (Figure 4b), $|B_z| < 1$ nT and $|B_y| < 1$ nT are used. As was expected, substorm onset latitudes appear to be moderately

Figure 4. Ionospheric substorm onset latitudes as a function of (a) IMF B_y for $|B_x| < 1$ nT and $|B_z| < 1$ nT and (b) B_x for $|B_y| < 1$ nT and $|B_z| < 1$ nT.

show each component of IMF effect, we have to limit the magnitude of the two other components to within ± 1 nT. Weak correlations are obtained for B_x ($r_m = -0.51$) and B_z ($r_m = -0.5$) as expected, but the correlation of the IMF B_y with the MLT location of onsets is much better ($r_m = -0.92$). The location of onset is found to shift toward early morning for negative B_y and toward early evening for positive B_y. Linear regression analysis indicates that for every 1 nT increase in B_y, onsets move westward by 0.16 hour of MLT (about $2.5°$ in longitude).

The x component of the IMF is expected to distort the Earth's dipole field lines in the x GSM direction on the basis of the "dipole plus uniform field" model; therefore the longitudinal location of substorm onsets (occurring mainly in the premidnight region) should have little response to the x component of IMF but have a strong response to the y component. Plotted in Figure 6 are the onset locations in MLT for different signs and different magnitudes of IMF B_x. It is found that for either sign of B_x the correlation becomes higher as the magnitude of B_x becomes larger. The most interesting finding is that different signs of B_x result in different signs of B_y correlation, which means that for a given B_y the sense of the MLT shift depends on the sign of B_x. For $B_x \ll 0$, onset locations shift toward early evening for $B_y < 0$ and toward early morning for $B_y > 0$. However, a slightly dominant B_y effect from a positive B_x is discernible, and it causes the overall B_y effect for all B_x (see Figure 5) to resemble those in Figures 6d-6f.

5. Seasonal Effect

To investigate seasonal effects in the location of auroral substorm onsets, we divide our database into different seasons centered around the equinoxes and solstices. Approximately, our database covers the full periods of winter, spring, and summer but just misses the fall season.

Figure 7 shows histograms of onset location in magnetic local time and magnetic latitude for the three surveyed seasons for which we have sufficient data. One can see from Figures 7a-7c that the peak onset location shifts toward early evening (2130 MLT) in summer and toward midnight (2300 MLT) in winter. The peak location of onsets for spring is intermediate to those of the solstitial periods. The difference in the peak onset location between summer and winter is ~ 1.5 hours, and the difference in the median location of onset is 1 hour of MLT. The result in the peak latitudinal location of onsets for the three seasons shown in Figures 7d-7f, however, remains the same. There is a small change in the average onset latitude from summer to winter. In winter the average onset latitude is highest, $\Lambda_m = 67.6°$, followed by summer, $\Lambda_m = 66.8°$, and spring, $\Lambda_m = 66.1°$.

Figure 5. Ionospheric substorm onset local times as a function of (a) IMF B_x, (b) IMF B_y, and (c) IMF B_z.

affected by the x component of IMF ($r_m = -0.66$) and not affected by the y component of IMF ($r_m = -0.05$).

4.2. Correlation of the Onset MLT With IMF

Figure 5 shows effects of the three IMF components on the MLT location of onsets in 2-nT bins. Again, in order to

6. Discussion

It has long been documented that auroral substorms take place preferentially in the premidnight region. Our statistical result, which is based on 648 auroral substorm onset events identified with global UVI images, indicated that the most probable onset location is 2230 MLT. The majority ($\sim 90\%$)
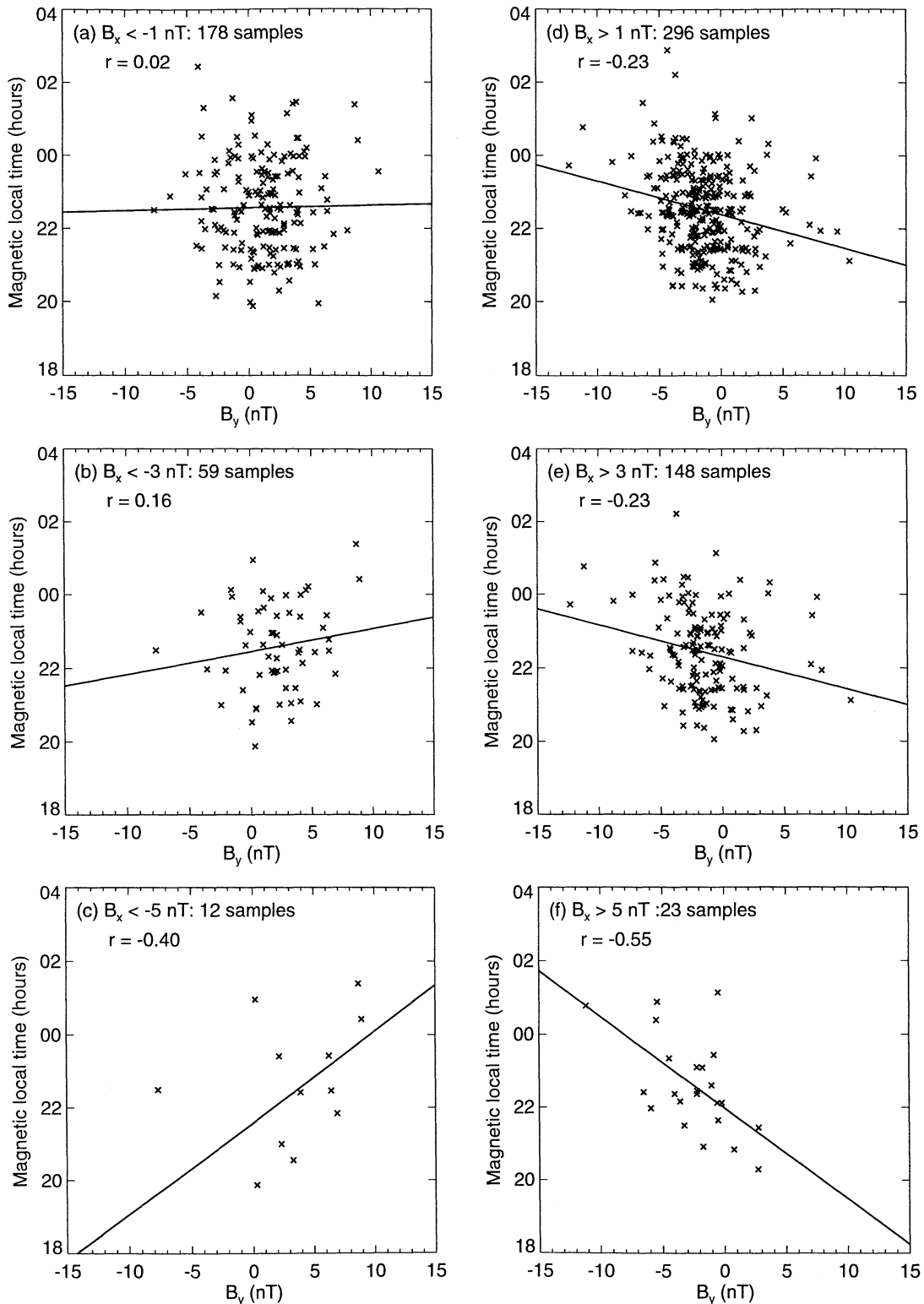
Figure 6. Dependence of MLT location of onset on IMF B_y for (a) IMF $B_x < -1$ nT, (b) $B_x < -3$ nT, (c) $B_x < -5$ nT, (d) $B_x < 1$ nT, (e) $B_x < 3$ nT, and (f) $B_x < 5$ nT.

of the auroral substorm onsets in our database occurred in the premidnight sector, and only ~9% of the total studied events occurred postmidnight. Our result is in surprisingly good agreement with those from much smaller studies using DE-1 [*Craven and Frank*, 1991] and Viking [*Henderson*

and Murphree, 1995] observations (see Table 1), although Viking results contain "pseudobreakups" in their database. The distribution of onset location in MLT is nearly symmetric, with a half-maximum width of ~3 hours in MLT centered around 2230 MLT. All of these results suggest that the
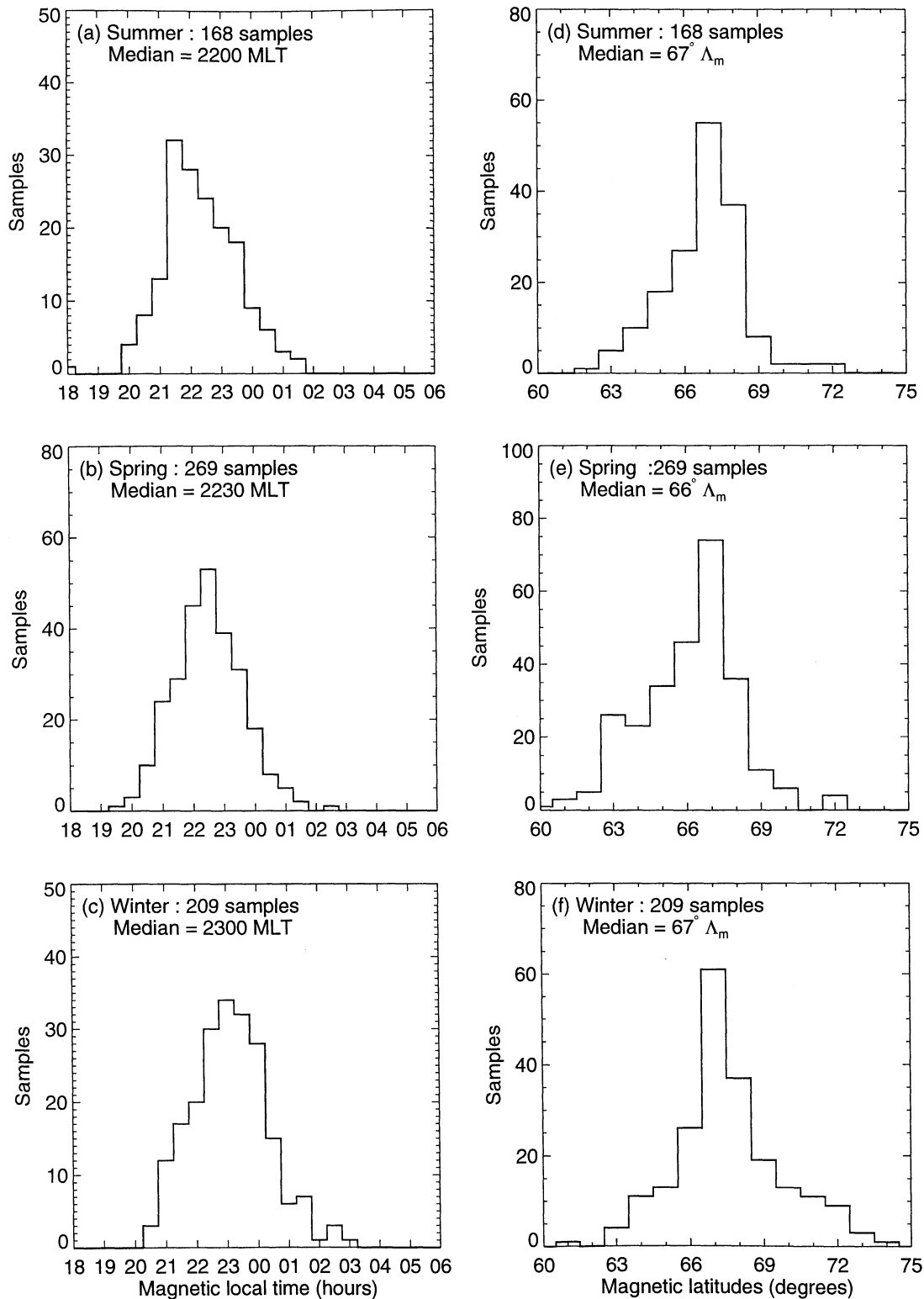
Figure 7. Histograms of seasonal distribution of auroral substorm onset location for three different seasons: summer (Figures 7a and 7d), spring (Figures 7b and 7e), and winter (Figures 7c and 7f).

location of auroral substorm onsets remains confined to the vicinity of 2230 MLT for a variety of external and/or internal conditions. Indeed, the typical auroral bulge location coincides with the location where intense discrete auroras are most probable [*Newell et al.*, 1996].

The distribution of onset latitudes is less symmetric but peaks sharply at $67°$ Λ_m, which accounts for 30% of total events studied. This result agrees well with observations from Viking [*Henderson and Murphree*, 1995] but is $\sim 2°$ higher than those from DE-1 reported by *Craven and Frank*

Table 1. Median Locations of Auroral Substorm Onset From Three Observations

	Samples	MLT (hours)	MLAT (Degrees)	References
DE-1	68	2250 (22.8)	65° (?)	*Craven and Frank* [1991]
Viking	133	2305 (22.8)	66.7°(65.8°)	*Henderson and Murphree* [1995]
Polar	648	2230 (22.7)	67° (66.6°)	present paper

Numbers in parentheses denote the average values.

[1991]. Note that the onset locations from DE-1 and Viking were calculated on the basis of the corrected geomagnetic (CGM) coordinate system, while ours were computed with the AACGM coordinate system. Theoretically, the AACGM coordinates are identical to the CGM coordinates for any point on the surface of Earth. At an auroral source height of 120 km, the difference is $< 0.5°$ in latitude in the auroral zone. Therefore this discrepancy in the onset latitude is probably not due to the different coordinate systems used. Section 4.1 shows that the orientation and magnitude of the IMF, in particular the IMF B_z, strongly influence onset latitudes. Since the DE-1 study used the least number of samples, its results are the most likely to be biased. Information about onset position can be used with a magnetic field model to infer the typical initiation site of a magnetospheric substorm in the magnetotail [*Murphree et al.*, 1993], but such work lies outside the scope of the present paper.

The IMF dependence of the onset location is consistent with current magnetospheric substorm theories. For instance, the fact that the z component of the IMF strongly controls the latitudinal location of onsets is consistent with the concept of substorm growth phase [*McPherron*, 1970], during which newly opened magnetic flux is being fed into the polar region through reconnection on the dayside and subsequently enlarges the size of polar cap [*Kauristie*, 1995]. It is important to note that the poleward border of the midnight oval is primarily controlled by substorms because the auroral surge after substorm onset expands poleward quickly even when B_z remains negative. Since auroral breakups usually, but not always, occur at the most equatorward arcs inside the diffusive oval [*Rostoker et al.*, 1980], the latitudinal location of onsets is closely related to the location of the equatorward edge of the main auroral oval in the midnight sector. Our least squares fit to the onset latitudes for $B_z < 0$ gives $\Lambda_m = 67.2° + 0.6\,B_z$ (nT), which is in good agreement with that reported by *Holzworth and Meng* [1984].

The response of the magnetosphere and ionosphere to the x and y components of the IMF has been widely studied. *Meng* [1979] fit circles to DMSP images of the auroral oval to determine displacements of the center location of polar cap as a function of the x and y components of the IMF. He showed that the Northern Hemisphere polar cap shifts duskward (dawnward) for $B_y < 0$ ($B_y > 0$) and sunward (tailward) for $B_x < 0$ ($B_x > 0$). Our results indicate a median correlation between the latitudinal location of substorm onsets and the x and y components of the IMF. In agreement with the results of *Meng* [1979], we found that substorm on-

sets tend to occur at higher latitudes for $B_x < 0$ than for $B_x > 0$. On the basis of a simple "dipole plus uniform field" picture and a typical Parker spiral configuration of IMF in the solar wind, *Cowley et al.* [1991] showed evidence of the oval dispalcement in the noon-midnight direction associated with the x component of the IMF. The sense of the shift in the longitudinal location of substorm onsets can also be consistent with the results of *Meng* [1979] because a slightly duskward (dawnward) shift of the oval can result in a westward (eastward) and equatorward (poleward) shift of the onset location (see Figure 5b). Note that a sunward (tailward) displacement of the polar cap center does not necessarily warrant a poleward (equatorward) movement of the midnight oval because the size of the oval may change in response to the IMF and other conditions during the course of displacement. On the basis of a physically plausible model and the consistency between the results of this study and those of Meng's, it is reasonable to conclude that the latitudinal location of the midnight oval is moderately correlated with the x and y components of the IMF, and it is also reasonable to suggest that ionospheric substorm onset locations move in harmony with the midnight oval, although the change in breakup locations in response to the IMF may be due to motion of the onset locations or of the entire oval.

The comparison of IMF B_y effects on substorm onset locations and the sharp reversal of ionospheric convection in the evening sector is somewhat complex. However, consistent with observations from radar *Ruohoniemi and Greenwald* [1995], both ionospheric features do indicate a systematic westward shift for $B_y > 0$ and an eastward shift for $B_y < 0$. This B_y effect is also controlled, but weakly, by the x component of the IMF: the location of breakups shifts toward early morning for a typical Parker spiral IMF and toward early local evening for an anti-Parker spiral IMF. Incidentally, our onset database shows an overall motion toward early evening for $B_y > 0$ and early morning for $B_y > 0$ for small B_x. We do not know whether this is typical or not and can provide no explanation in the absence of any theoretical models. Note that IMF B_x was not considered in the work of *Ruohoniemi and Greenwald* [1995]. It is difficult to conceive of a mechanism for the asymmetric B_y effect due to the polarity of B_x without considering antiparallel merging [e.g., *Crooker*, 1979; *Heelis*, 1984]. According to the antiparallel merging model, the merging rate is highest where the mangetic shear is greatest. Therefore the preferred merging site is controlled by both the x and y components of IMF: for $B_x > 0$ ($B_x < 0$) the preferred merging side is

in the north (south) hemisphere on the duskside for $B_y > 0$ ($B_y < 0$) and on the dawnside for $B_y < 0$ ($B_y > 0$). Interestingly, the MLT location of auroral breakup appears to respond to the x and y components of IMF in a similar way, suggesting that substorm onset locations are controlled by reconnection on the dayside.

Seasonal effects represent another interesting result from this study. A systematic change in the onset locations from early evening toward midnight is observed as the season changes from winter through spring to summer. Of course, the seasonal effect on the MLT location of onset may be due to a nonuniform distribution of IMF in each season. To test this hypothesis, Table 2 presents the three components of the hourly-averaged IMF taken at onset intervals for the three seasons. In summer, $\langle B_x \rangle = 0.37$ nT and $\langle B_y \rangle = -0.33$ nT, leading us to expect more substorms after 2230 MLT. In winter, $\langle B_x \rangle = 0.07$ nT and $\langle B_y \rangle = -0.17$ nT, leading us to expect more substorms before 2230 MLT. Neither prediction agrees with the observed seasonal effect shown in Figures 6a-6c. In fact, these average values for the IMF in both seasons are quite small, and the IMF bias should not even be a significant factor. On the other hand, the latitudinal onset locations do reflect the average z component of the IMF quite well. For example, the average IMF B_z is smallest in spring and largest in winter, which is consistent with the observed shifts in onset latitudes. This result resembles that reported by Ruohoniemi and Greenwald [1995], who analyzed HF radar data observed from Goose Bay and showed that the zonal flow reversal occurs earlier in local time for summer than for winter. On the basis of our results, it is reasonable to argue that the locations of the HD and onset arcs are closely related, as was reported by many previous case studies [e.g., Koskinen and Pulkkinen, 1995, and references therein].

Thus both IMF orientation and season control the MLT location of onsets. The combined B_y and seasonal effect is shown in Figures 8a and 8b for $|B_x| < 1$ nT and $B_z < -1$ nT, and the combined B_x and seasonal effect is shown in Figures 8c and 8d for $|B_y| < 1$ nT and $B_z < -1$ nT. The figure somewhat contradicts our previous result; the MLT location of onsets is not likely controlled by B_x ($r = -0.05$ for winter and $r = -0.16$ for summer) but by B_y ($r = -0.49$ for winter and $r = -0.41$ for summer). The effect is only moderate, however. One possible explanation is that B_x is not large enough to have significant effects; more samples are needed to validate this line of argument. During winter a positive B_y causes onsets to occur at earlier local times, while a positive B_y causes onsets to occur at later local times. This combined result is consistent with the seasonal and B_y effects on the reversal of the dusk cell zonal flow on the nightside

as reported by Ruohoniemi and Greenwald [1995]. However, during summer the effect of B_y becomes opposite and cannot be consistent with their convection result obtained from ground radars. A close examination of Figure 4 of Ruohoniemi and Greenwald [1995] indicates that the longitude of the nightside flow reversal boundary is actually about the same for both signs of B_y in summer. Incidentally, the slope of the fitted line is smaller for the onset local time, as shown in Figure 8b, indicating that B_y effect is probably weaker in summer. Table 3 shows the combined seasonal and B_y effects. In agreement with the radar results, the average onset local time is earliest (2200 MLT) for $B_y > 0$ and summer and latest (2330 MLT) for $B_y < 0$ and winter; onset local times fall between the two extremes for the other two combinations.

It is interesting that the westward auroral electrojet index AL, normalized by a modified energy coupling function, $(| - B_z|+0.5)V_{sw}^2$, presents similar IMF B_y and seasonal effects: during Northern Hemisphere summer ($\chi > 0$), the normalized AL value is about twice as great for $B_y < 0$ than for $B_y > 0$. During Northern Hemisphere winter ($\chi < 0$), the normalized AL value is about twice as great for $B_y > 0$ than for $B_y < 0$ [Murayama et al., 1980]. There is an overall decrease in the normalized AL from summer to winter. This combined IMF B_y tilt angle effect has been attributed to antiparallel merging by Crooker [1979]. When $\chi > 0$, reconnection occurs predominantly in the northern cusp [Alexander and Kaiser, 1976] and occurs on the duskside of the cusp for $B_y > 0$ and on the dawnside for $B_y < 0$. In contrast, when $\chi > 0$, reconnection occurs predominantly on the dawnside for $B_y > 0$ and on the duskside for $B_y < 0$. As a consequence, the enhancement of the westward electrojet is strongly associated with dawnside reconnection. If the location of the HD is controlled by the relative intensity of the eastward and westward electrojets, an enhancement of the westward electrojet may cause the HD to shift toward early evening, provided the eastward electrojet remains relatively constant. On the basis of this argument, the HD will move to early evening (morning) for $B_y > 0$ and early morning (evening) for $B_y < 0$ in winter (summer). Since the location of onset arcs and HD appears to be closely correlated, onset locations should move in a similar manner, which is consistent with our results shown in Figures 8a and 8b. The overall increase in normalized AL from winter to summer can also be used to infer an average onset location occurring earlier in local time for summer than for winter, as indicated in Figure 5.

The average onset latitude is least in spring; this is because the magnetosphere is usually slightly more active in spring than in summer and winter [e.g., Russell and McPherron, 1973]. The average onset latitude was found to be highest in winter; however, the winter-summer difference is only $\sim 1°$. We suggest that this may be due to changes in the Earth's dipole angle with respect to the IMF. In general, the latitudinal location of the cusp is $\sim 4°$ lower in the winter hemisphere than in the summer hemisphere owing to the effect of dipole tilt [Burch, 1972; Newell and Meng, 1989]. If the nightside auroral oval moves systematically with the

Table 2. Seasonal Averages of IMF in nT

	$\langle B_x \rangle$	$\langle B_y \rangle$	$\langle B_z \rangle$
Summer	0.37	-0.33	-0.81
Spring	1.29	-0.93	-0.96
Winter	0.07	0.17	-0.42
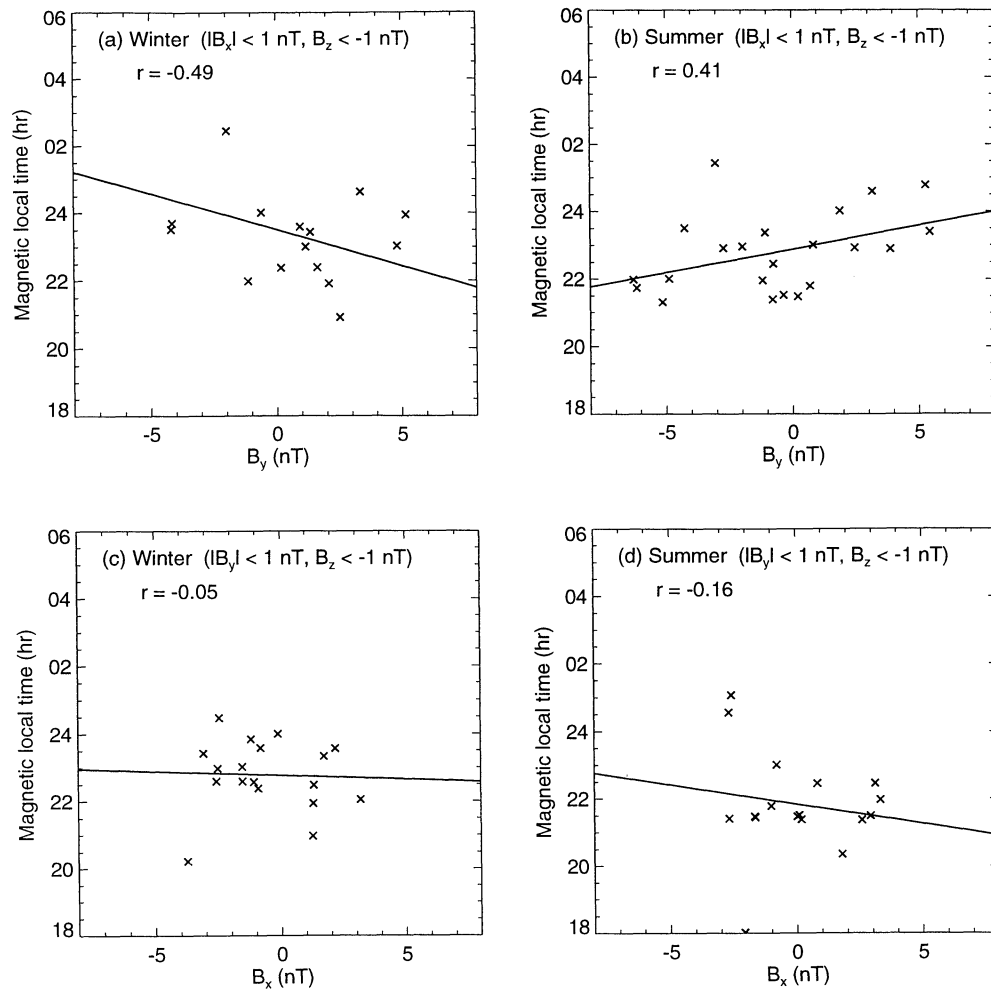
Figure 8. Ionospheric substorm onset MLT locations as a function of IMF B_y for (a) winter and (b) summer for $|B_x| < 1$ nT and of IMF B_x for (c) winter and (d) summer for $|B_y| < 1$ nT. $B_z < -1$ nT for all cases.

dayside cusp seasonally, as predicted by *Voigt* [1976] on the basis of a theoretical consideration for the boundary between open and closed field lines, then one would expect to observe substorm onset at higher latitude in winter than in summer. However, the seasonal change in the onset latitudes is less dramatic compared to the cusp.

The IMF and seasonal effects on the MLT location of auroral breakup implies that the onset arcs are not conjugate. Since auroral arcs are formed by accelerated electrons in the near-Earth magnetosphere, asymmetries in the auroral arcs seen in the two hemispheres can arise from asymmetries in geomagnetic field topology, electric potential distribution, and field-aligned currents that flow into and out of the ionosphere relative to the equatorial plane. However, these factors are usually closely related and can be associated with an extra B_y in the magnetosphere. Penetrations of the IMF B_y component into the plasma sheet [*Wing et al.*, 1995; *Lui*, 1984] have been used to explain observations of nonconjugate discrete aurora [*Stenbaek-Nielsen and Otto*, 1997]. The penetration of the IMF B_y component provides a means to distort the nightside geomagnetic field structure in a way such that a field line's ionospheric footprint in the North-

ern Hemisphere shifts eastward relative to the other end of ionospheric footprint for $B_y < 0$ and vice versa. Therefore negative B_y will cause onset arcs to occur at a later magnetic local time in the Northern Hemisphere than positive B_y, in good agreement with our result shown in Figure 5b.

Recent results indicated that ionospheric conductivity may play an important role in forming the discrete aurora. *Newell et al.* [1996] reported that intense discrete auroral arcs are more common in darkness than in sunlight. Auroral luminosities in the UV band are more intense in the dark than the sunlit ionosphere [*Liou et al.*, 1997]. As a consequence, a net current on the nightside out of the winter hemisphere and into the summer hemisphere is implied, and a residual

Table 3. Average Onset MLT Sorted by Season and IMF B_y

	Summer	Winter
$B_y > 1$ nT	22.0	23.0
$B_y < -1$ nT	22.6	23.5

B_y which is independent of IMF is expected earthward of the net current region [*Newell et al.*, 1999]. On the basis of our results, an eastward shift of the onset location during the northern hemispheric winter requires a negative B_y. This negative B_y can be generated by the net current that flows out of the winter hemisphere. By the same reasoning, a positive B_y resulting from a net current into the summer hemisphere can move the onset location westward. However, the existence of the net current has not been confidently identified.

The geosynchronous magnetic field may respond to variations in the x component of the IMF [*Hughes and Cowley*, 1986]. It is conceivable that an extra B_x in the magnetosphere can displace both ends of the auroral field lines latitudinally such that they map to different conductivity regions, such as one end inside the oval and the other end outside the oval. A net current that flows from a high-conductance hemisphere into a low-conductance hemisphere is expected. A residual B_y is also expected and is able to move onset locations longitudinally. However, the most dramatic variations in the geosynchronous magnetospheric are usually associated with the well-known magnetic field line stretching and dipolarization during substorm periods. Therefore whether the IMF B_x can penetrate into the magnetospher is less clear (S. Wing, private communication, 2000), and whether the IMF B_x can change the MLT location of auroral breakup in this fashion is not so obvious.

7. Summary

In this paper we have investigated IMF and seasonal effects upon the location of auroral substorm onsets using simultaneous the Polar UVI images and Wind IMF observations. Several notable findings, based on 648 onsets, were listed as follows: (1) The most probable onset location lies at 2230 MLT and $67°\Lambda_m$, with more than 90% of onsets taking place in the premidnight sector. (2) IMF B_z controls latitudinal onset locations, with $\Lambda_m = \Lambda_0 + 0.6\ B_z$ (nT). (3) IMF B_x moves the auroral oval sunward or antisunward, opposite to the orientation of B_x, and therefore controls event latitudes. (4) The onset latitude is least when a toward (the Sun) IMF is combined with a southward IMF B_z and greatest for an away IMF and a northward IMF B_z. (5) Substorm onset occurs, on average, ~1.5 hours earlier in local time in summer than in winter. (6) Substorm onset tends to occur earlier in local time for $B_y > 0$ than for $B_y < 0$. (7) A large value of IMF B_x may also affect the onset local times in a way such that the location of breakups shifts toward early morning for a typical Parker spiral IMF and toward early local evening for an anti-Parker spiral IMF.

Some general conclusions can also be made here on the basis of consistencies between our results and those previously reported. (1) The auroral breakup location is confined to a narrow premidnight region which is topologically fixed in the oval coordinate system. (2) Auroral breakups most likely take place in regions of strong ionospheric flow shear. (3) Auroral breakup is not conjugate.

References

Akasofu, S.-I., The development of the auroral substorm, *Planet. Space Sci.*, *12*, 273, 1964.

Alexander, J. K., and M. L. Kaiser, Terrestrial kilometric radiation, 1, spatial structure studies, *J. Geophys. Res.*, *81*, 5984, 1976.

Arnoldy, R. L., Signature in the interplanetary medium for substorms, *J. Geophys. Res.*, *76*, 5189, 1971.

Baker, K. B., and S. Wing, A new coordinate system for conjugate studies at high latitudes, *J. Geophys. Res.*, *94*, 9139, 1989.

Bargatze, L. F., R. L. McPherron, and D. N. Baker, Solar wind-magnetosphere energy input functions, in *Solar Wind-Magnetosphere Coupling*, edited by Y. Kamide and J. A. Slavin, pp. 101-109, Terra Sci., Tokyo, 1986.

Baumjohann, W., J. Pellinen, H. J. Opgenoorth, and E. Nielsen, Joint two-dimensional observations of ground magnetic and ionospheric electric fields associated with auroral zone currents: Current systems associated with local auroral breakups, *Planet. Space Sci.*, *29*, 431, 1981.

Burch, J. L., Precipitation of low-energy electrons at high latitudes: Effects of interplanetary magnetic field and dipole tilt angle, *J. Geophys. Res.*, *77*, 6696, 1972.

Cowley, S. W. H., A qualitative study of the reconnection between the earth's magnetic field and an interplanetary magnetic field of arbitrary orientation, *Radio Sci.*, *8*, 903, 1973.

Cowley, S. W. H., J. P. Morelli, and M. Lockwood, Dependence of convective flows and particle precipitation in the high-latitude dayside ionosphere on the x and y components of the interplanetary magentic field, *J. Geophys. Res.*, *96*, 5557, 1991.

Craven, J. D., and L. A. Frank, Diagnosis of auroral dynamics using global auroral imaging with emphasis on large-scale evolution, in *Auroral Physics*, edited by C.-I Meng, M. J. Rycroft, and L. A. Frank, pp. 273-297, Cambridge Univ. Press, New York, 1991.

Crooker, N. U., Dayside merging and cusp geometry, *J. Geophys. Res.*, *84*, 951, 1979.

de la Beaujardiere, O., D. Alcayde, J. Fontanari, and C. Leger, Seasonal dependence of high-latitude electric fields, *J. Geophys. Res.*, *96*, 5723, 1991.

Dungey, J. W., Interplanetary magnetic field and the auroral zones, *Phys. Rev. Lett.*, *6*, 47, 1961.

Elphinstone, R. D., J. S. Murphree, and L. L. Cogger, What is a global auroral substorm?, *Rev. Geophys.*, *34*, 169, 1996.

Harang, L., The mean field of disturbance of polar geomagnetic storms, *J. Geophys. Res.*, *51*, 353, 1946.

Heelis, R. A., The effects of interplanetary magnetic field orientation on dayside high-latitude ionospheric convection, *J. Geophys. Res.*, *89*, 2873, 1984.

Henderson, M. G., and J. S. Murphree, Comparison of viking onset locations with the predictions of the thermal catastrophe model, *J. Geophys. Res.*, *100*, 21,857, 1995.

Heppner, J. P., Polar cap electric field distribution related to the interplanetary magnetic field direction, *J. Geophys. Res.*, *77*, 4877, 1972.

Holzworth, R. H., and C.-I. Meng, Mathematical representation of the auroral oval, *Geophys. Res. Lett.*, *2*, 377, 1975.

Holzworth, R. H., and C.-I. Meng, Auroral boundary variations and the interplanetary magnetic field, *Planet. Space Sci.*, *32*, 25, 1984.

Hughes, W. J., and S. W. H. Cowley, Observation of IMF-associated magnetic field perturbations in the gsm x component at the geostationary orbit, in *Solar Wind-Magnetosphere Coupling*, edited by Y. Kamide and J. A. Slavin, pp. 691-695, Terra Sci., Tokyo, 1986.

Kauristie, K., Statistical fits for auroral oval boundaries during the substorm sequence, *J. Geophys. Res.*, *100*, 21,885, 1995.

Koskinen, H. E. J., and T. I. Pulkkinen, Midnight velocity shear zone and the concept of harang discontinuity, *J. Geophys. Res.*, *100*, 9539, 1995.

Liou, K., P. T. Newell, C.-I. Meng, M. Brittnacher, and G. Parks, Synoptic auroral distribution: A survey using Polar ultraviolet imagery, *J. Geophys. Res.*, *102*, 27,197, 1997.

Liou, K., P. T. Newell, C.-I. Meng, M. Brittnacher, and G. Parks, Characteristics of the solar wind controlled auroral emissions, *J. Geophys. Res.*, *103*, 17,543, 1998.

Lui, A. T. Y., Characteristics of the cross-tail current in the Earth's magnetotail, in *Magnetospheric Currents, Geophys. Monogr. Ser.*, vol. 28, edited by T. A. Potemra, pp. 158-170, AGU, Washington, D. C., 1984.

Lyons, L. R., A simple model for polar cap convection patterns and generation of theta auroras, *J. Geophys. Res.*, *90*, 1561, 1985.

McPherron, R. L., Growth phase of magnetospheric substorms, *J. Geophys. Res.*, *75*, 5992, 1970.

Meng, C.-I., Polar cap variations and the interplanetary magnetic field, in *Dynamics of the Magnetosphere*, edited by S.-I. Akasofu, pp. 23-46, D. Reidel, Norwell, Mass., 1979.

Meng, C.-I., B. Tsurutani, K. Kawasaki, and S.-I. Akasofu, ross-correlation analysis of the ae index and the interplanetary magnetic field B_z component, *J. Geophys. Res.*, *78*, 617, 1973.

Murayama, T., T. Aoki, H. Nakai, and K. Hakamada, Empirical formula to relate the auroral electrojet intensity with interplanetary parameters, *Planet. Space Sci.*, *28*, 803, 1980.

Murphree, J. S., R. D. Elphinstone, M. G. Henderson, L. L. Cogger, and D. J. Hearn, Interpretation of optical substorm onset observations, *J. Atmos. Terr. Phys.*, *55*, 1159, 1993.

Nakai, H., The northern and southern auroral ovals in response to the IMF B_y component, *Geophys. Res. Lett.*, *14*, 1162, 1987.

Newell, P. T., and C.-I. Meng, Dipole tilt angle effects on the latitude of the cusp and cleft/low-latitude boundary layer, *J. Geophys. Res.*, *94*, 6949, 1989.

Newell, P. T., C.-I. Meng, and K. M. Lyons, Suppression of discrete aurorae by sunlight, *Nature*, *381*, 766, 1996.

Newell, P. T., S. Wing, K. Liou, and C.-I. Meng, Interhemispherical current implied by seasonal auroral variation: An explanation for the local time shift in substorm onset, paper presented at Chapman Conference on Magnetospheric Current Systems, AGU, Kona, Hawaii, 1999.

Rich, F. J., and M. Hairston, Large-scale convection patterns observed by dmsp, *J. Geophys. Res.*, *99*, 3827, 1994.

Robinson, R. M., and R. R. Vondrak, Electrodynamic properties of auroral surges, *J. Geophys. Res.*, *95*, 7819, 1990.

Rodger, A. S., S. W. H. Cowley, M. J. Brown, M. Pinnock, and D. A. Simmons, Dawn-dusk (y) component of the interplanetary magnetic field and the local time of the harang discontinuity, *Planet. Space Sci.*, *32*, 1021, 1984.

Rostoker, G. A., H.-L. Lam, and W. D. Hume, Response time of the magnetosphere to the interplanetary electric field, *Can. J. Phys.*, *50*, 544, 1972.

Rostoker, G. A., S.-I. Akasofu, J. Foster, R. A. Greenwald, A. T. Y. Lui, Y. Kamide, K. Kawasaki, R. L. McPherron, and C. T. Russel, Magnetospheric substorms: Definition and signatures, *J. Geophys. Res.*, *85*, 1663, 1980.

Ruohoniemi, J. M., and R. A. Greenwald, Observations of IMF and seasonal effects in high-latitude convection, *Geophys. Res. Lett.*, *22*, 1121, 1995.

Russell, C. T., and R. L. McPherron, Semiannual variation of geomagnetic activity, *J. Geophys. Res.*, *78*, 92, 1973.

Starkov, G. V., Y. I. Feldstein, and F. Shevnina, Auroras on the dayside of the oval during substorms, *Geomagn. Aeron.*, *11*, 72, 1971.

Stenbaek-Nielsen, H. C., and A. Otto, Conjugate auroras and the interplanetary magnetic field, *J. Geophys. Res.*, *102*, 2223, 1997.

Stern, D. P., A study of the electric field in an open magnetospheric model, *J. Geophys. Res.*, *78*, 7292, 1973.

Torr, M. R., et al., A far ultraviolet imager for the international solar-terrestrial physics mission, *Space Sci. Rev.*, *71*, 329, 1995.

Voigt, G. H., Influence of magnetospheric parameters on geosynchronous field characteristics, last closed field lines and dayside neutral points, in *The Scientific Satellite Programme During the International Magnetospheric Study*, edited by K. Knott and B. Battrick, pp. 381-396, D. Reidel, Norwell, Mass., 1976.

Vorobjev, V. G., . G. V. Starkov, and Y. I. Feldstein, The auroral oval during the substorm development, *Planet. Space Sci.*, *24*, 955, 1976.

Wing, S., P. T. Newell, D. G. Sibeck, and K. B. Baker, A large statistical study of the entry of interplanetary magnetic field y-component into the magnetosphere, *Geophys. Res. Lett.*, *22*, 2083, 1995.

M. Brittnacher and G. Parks, Geophysics Program, University of Washington, Seattle, WA 98195. (britt@geophys.washington.edu; parks@geophys.washington.edu)

K. Liou, C.-I Meng, P. T. Newell, and D. G. Sibeck, The Johns Hopkins University Applied Physics Laboratory, Laurel, MD 20723. (Kan.Liou@jhuapl.edu; Ching.Meng@jhuapl.edu; Patrick.Newell@jhuapl.edu; David.Sibeck@jhuapl.edu)